Molecular dynamics study of plastic deformation mechanism in Cu/Ag multilayers*

Yuan-Yuan Tian(田圆圆)[1,2], Jia Li(李甲)[1,2], Ze-Ying Hu(胡泽英)[1,2], Zhi-Peng Wang(王志鹏)[1,2], and Qi-Hong Fang(方棋洪)[1,2,†]

[1] State Key Laboratory of Advanced Design and Manufacturing for Vehicle Body, Hunan University, Changsha 410082, China
[2] College of Mechanical and Vehicle Engineering, Hunan University, Changsha 410082, China

(Received 24 July 2017; revised manuscript received 24 August 2017; published online 20 October 2017)

The plastic deformation mechanism of Cu/Ag multilayers is investigated by molecular dynamics (MD) simulation in a nanoindentation process. The result shows that due to the interface barrier, the dislocations pile-up at the interface and then the plastic deformation of the Ag matrix occurs due to the nucleation and emission of dislocations from the interface and the dislocation propagation through the interface. In addition, it is found that the incipient plastic deformation of Cu/Ag multilayers is postponed, compared with that of bulk single-crystal Cu. The plastic deformation of Cu/Ag multilayers is affected by the lattice mismatch more than by the difference in stacking fault energy (SFE) between Cu and Ag. The dislocation pile-up at the interface is determined by the obstruction of the mismatch dislocation network and the attraction of the image force. Furthermore, this work provides a basis for further understanding and tailoring metal multilayers with good mechanical properties, which may facilitate the design and development of multilayer materials with low cost production strategies.

Keywords: Cu/Ag multilayers, nanoindentation, molecular dynamics, interface

PACS: 68.90.+g, 61.46.–w, 62.25.–g, 67.30.hp **DOI:** 10.1088/1674-1056/26/12/126802

1. Introduction

The structure formed by alternately stacking two or more different metal materials is called metal multilayers. Compared with bulk pure metals, metal multilayers have high strength,[1–3] good mechanical stability,[4] strong ductility and fracture toughness.[5–8] Due to excellent performances of metal multilayers, they have been widely used in various fields.[9,10] For example, Cu/Ag multilayers are popularly used in engineering fields because of their strong antioxidative property, good electrical and thermal conductivity, and high strength.[11–13]

In order to develop metal multilayers, it is necessary to understand the plastic deformation mechanism of metal multilayers in detail. At present, there is a great deal of research about the plastic deformation mechanism of metal multilayers, such as Hall-Petch relations,[14,15] Koehler's image force theory[16,17] and Orowan's relation.[18] They show consistently that the plastic deformation of metal multilayers is closely related to the interface.

In our previous work, the interface effects have been investigated by theoretical models.[19–21] In addition, we also conducted a series of machining nano-material processes by MD simulation[22–24] because of its advantage in observing the deformation processes on a nanometer scale. Furthermore, MD simulation is also a viable tool to reveal the interface effect on the plastic deformation of metal multilayers, which involves the interaction between the interface and dislocations. For example, Shao and Medyanik studied the dislocation-interface interaction by MD simulation of nanoindentation in a Cu–Ni bilayer, and showed that the shear of interface results in the interfacial stacking fault formation.[25] Recently, Zhang *et al.* investigated the interface-dependent nanoscale frictions in Cu using MD simulation, and found that the dislocation motion was blocked by grain boundary results in the strain hardening of the bicrystals.[26] In addition, Cao *et al.* showed that the semi-coherent interface makes the glide dislocation difficult to cross the interface.[27] Although lots of studies have been performed to investigate the interface effect on the plastic deformation of metal materials by using MD simulation, the plastic deformation mechanism of Cu/Ag multilayers has hardly been studied on a nanoscale.

The nanoindentation experiments show that the interface plays a vital role in the plastic deformation of Cu/Ag multilayers.[28–31] However, these experiments cannot present more details about the interface effect on a nanoscale, due to the dependence on the experimental equipments such as scanning electron microscopy (SEM) and transmission electron microscopy (TEM).[32–36] Therefore, it is necessary to characterize the interface effect on the plastic deformation of Cu/Ag multilayers during nanoindentation by MD simulation.

In this paper, by using the MD simulation we conduct the nanoindentations of Cu/Ag multilayers and bulk single-

*Project supported by the National Natural Science Foundation of China (Grant Nos. 11572118 and 11372103), the Hunan Provincial Science Fund for Distinguished Young Scholars, China (Grant No. 2015JJ1006), and the National Key Research and Development Program of China (Grant No. 2016YFB0700300).

†Corresponding author. E-mail: fangqh1327@hnu.edu.cn

© 2017 Chinese Physical Society and IOP Publishing Ltd

crystal Cu with the use of the embedded atom method (EAM) potential function equation from Wadley *et al.*[37] The simulation results show the interface effect on the dislocation motion, which provides an effective basis for the analysis of the plastic deformation mechanism of Cu/Ag multilayers. The rest of this paper consists of the following parts. Firstly, the MD models and analytical methods are described in detail in the second part. The nanoindentation processes of bulk single-crystal Cu and Cu/Ag multilayers are analyzed in the third part. Finally, the plastic deformation mechanism of Cu/Ag multilayers is determined by analyzing the morphology and motion of dislocations and the indentation force curves.

2. MD models and analytical methods

2.1. Establishment of three-dimensional models

Figure 1(a) shows a three-dimensional model to simulate the nanoindentation process of Cu/Ag multilayers. In this model, the indenter is a spherical diamond structure containing 47244 atoms with a radius of 4 nm and a velocity of 20 m·s^{-1}. The multilayers consisting of Cu nanofilm and Ag matrix have a size of 20, 20, and 12 nm in the X, Y, and Z directions. The Ag matrix containing 211 288 Ag atoms has a thickness of 8.9 nm, and the thickness of Cu nanofilm containing 104 729 Cu atoms is 3 nm. The three crystal orientations corresponding to the positive directions of the three-dimensional axes x, y, and z are $[1\bar{1}0]$, $[11\bar{2}]$, and [111] in the multilayers,[38] respectively. To eliminate the influence of the boundary, the x and y directions are set to be the periodic boundary condition. The lower surface is set to be the fixed boundary condition to prevent the model from motioning, and the upper surface contacting the indenter is set to be a free surface. According to the different positions of atoms in the multilayers, the atoms are divided into three categories, i.e., boundary atoms, thermostat atoms and Newtonian atoms. The boundary atoms located on the lower surface of the multilayers keep stationary to prevent the multilayers from motioning in the nanoindentation process.[39,40] The temperature of thermostat atoms next to boundary atoms is always maintained at 293 K by adjusting the velocity of the atoms once every five time steps during the simulation. The other atoms are Newtonian atoms. The movements of the Newtonian and thermostat atoms each follow Newton's classical second law, and the equations of motion are determined by the Velocity-Verlet numerical integration algorithm.

Lattice constants of fcc-Cu and fcc-Ag are 3.61 Å and 4.08 Å,[41] respectively. Therefore, their lattice mismatch is about 13%. A semi-coherent interface exists in Cu/Ag multilayers because of the lattice mismatch. Figure 1(b) indicates that the mismatch dislocations are periodically distributed as a network structure on the interface. In addition, figure 1(c) shows the model including a bulk single-crystal Cu.

The interactions between the atoms are the same in the two models, and divided into three categories. The interactions between Cu atoms and Ag atoms (Cu–Ag), between Cu atoms (Cu–Cu) and between Ag atoms (Ag–Ag) are described by the EAM potential because of its reliability.[24,41–43] The Morse potential exists between Cu atoms and diamond atoms (Cu–C).[40,44–46] There is no interaction between diamond atoms (C–C), and the indenter is seen as a rigid body because of its larger stiffness than Ag and Cu metals. Both simulation processes are composed of two stages: the relaxation stage and indentation stage. The Cu/Ag multilayers and bulk single-crystal Cu first undergo the steepest descent energy minimization at 293 K, and then are run for 100 ps under the isothermal-isobaric NVE ensemble in the relaxation stage. The two equilibrium configurations are obtained, and the equilibrium interface appears in Cu/Ag multilayers. After that, the indenter penetrates the Cu/Ag multilayers and bulk single-crystal Cu uniformly along the Z axis negative direction, respectively.

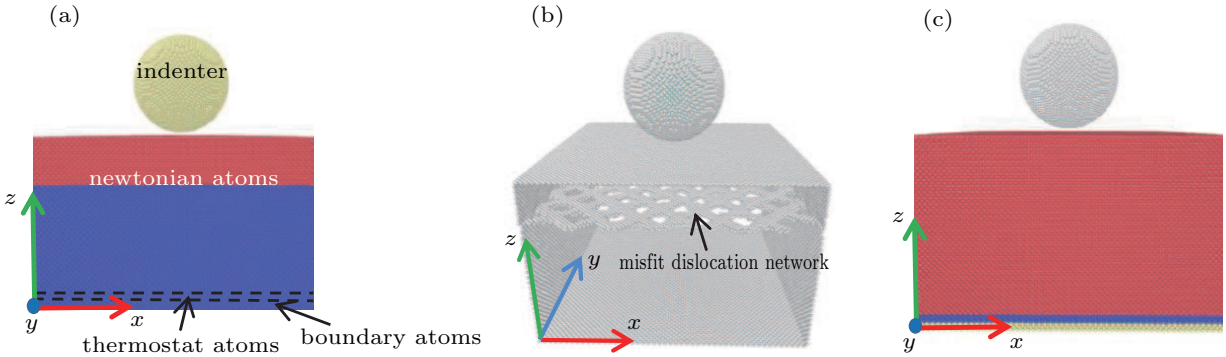


Fig. 1. (color online) MD simulation model of (a) Cu/Ag multilayers, (b) Cu/Ag multilayers with fcc atoms hidden, and (c) bulk single-crystal Cu.

2.2. Structural analysis methods

The two simulation processes are completed by the classical MD code LAMMPS, and the time step is 1 fs.[47] In order to obtain the microstructure of a certain stage of the model to facilitate the analysis of MD data, we use OVITO, a visualization tool.[48] In addition, the common neighbor analysis (CNA) method is used to effectively analyze the internal defects of the materials in the nanoindentation processes. Differ-

ent types of atoms are shown in different colors. In this paper, the fcc structural atoms are in green; the hcp structural atoms are in red, which form the stacking faults; the atoms in the dislocation nucleation are shown in blue; other defective atoms and surface atoms are in white.[49]

3. Results

In order to reveal the plastic deformation mechanism of Cu/Ag multilayers, figures 2 and 3 show the evolutions of the internal defects in the bulk single-crystal Cu and Cu/Ag multilayers in the nanoindentation process. The fcc atoms in green are hidden and only defective atoms are displayed to facilitate the observation of the dislocation morphologies.

Figure 2(a) shows the steady state before the indenter penetrates bulk single-crystal Cu. When the indenter reaches the critical depth for the yielding of bulk single-crystal Cu, the dislocations nucleate and propagate along the activated {111} plane as described in Fig. 2(b). With increasing indentation depth, another {111} plane is activated, and the dislocations are internally emitted from the free surface of the bulk along the two slipping planes to form V-shaped dislocations [50] (see Fig. 2(c)). As the indenter continues to penetrate the bulk, the stresses accumulated inside the bulk increase. The other two {111} planes are also activated and the dislocations propagate on the adjacent {111} planes, resulting in the dislocation intersections and dislocation loops. In addition, dislocation loops also propagate along the four {111} planes to form prism dislocation structures, see Fig. 2(d). With the indenter penetrating bulk single-crystal Cu, the high local stresses in the region of the indenter are produced. The dislocation loops sequentially are emitted into the interior of the bulk, and multiple dislocation loops appear in the bulk. Finally, the loops disappear in the lower surface as the plastic strain energy is released as shown in Fig. 2(e). Figure 2 indicates that the plastic deformation of bulk single-crystal Cu is controlled by the dislocation nucleation and propagation, and the plastic strain energy is released by the dislocation loops in the nanoindentation process.

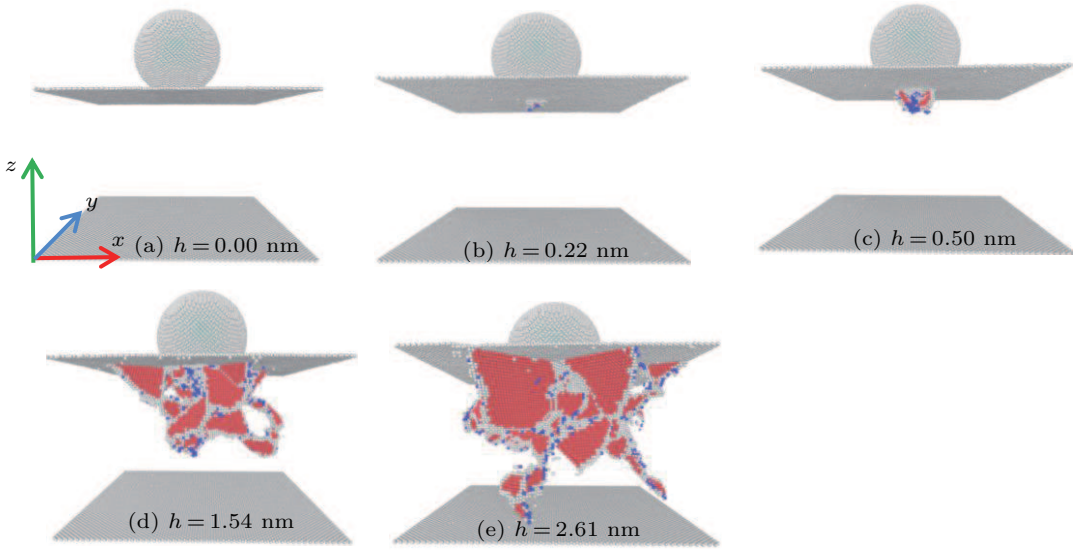


Fig. 2. (color online) Evolution processes of internal defects in bulk single-crystal Cu in the nanoindentation process.

Figure 3(a) shows the steady state before the indenter penetrates Cu/Ag multilayers. When the indenter reaches the critical depth for the yielding of Cu/Ag multilayers, the dislocations nucleate and are emitted from the top surface to the interface along the active {111} plane. The evolution of the internal defects of Cu/Ag multilayers is similar to that of bulk single-crystal Cu during the incipient plastic deformation (Fig. 3(b)). However, due to the dislocations piling up at the interface,[38] the mismatch dislocation network deforms, which causes the dislocations to nucleate and be emitted from the interface to the Cu nanofilm along the newly activated {111} planes (Fig. 3(c)). In addition, by comparing Figs. 3(c) and 3(d), the pre-existing dislocation continues to slip along the glide plane when the fresh dislocation propagates along the newly activated glide plane, which indicates that after the fresh dislocation nucleates from the interface, its subsequent propagation along impinging pre-existing dislocation is a slip of the fresh dislocation, not a bounce back phenomenon of the pre-existing dislocation.

With increasing indentation depth, more dislocations are emitted continuously from the top surface to the interface. Figure 3(e) shows the dislocation pile-up at the interface, because the interface hinders the dislocations from motioning.[26,27] In addition, the dislocation pile-up increases the movement resistance of the indenter, therefore, the load should be increased to maintain the uniform velocity of the indenter. As the indenter continues to penetrate Cu/Ag multilayers, the mismatch dislocation network deforms more seriously with the increase of interface stress and interface energy. In order to release the interface energy, more dislocations nucleate from the interface

and are emitted into the Cu nanofilm and Ag matrix[51] as displayed in Fig. 3(e). The dislocations propagate along the two activated {111} planes in the Ag matrix (Fig. 3(f)). Due to the increase of the indentation depth, the dislocation intersections appear in the Ag matrix with the dislocation propagating in the matrix along the four activated planes (Fig. 3(g)). Figure 3(h) shows the stacking faults in the Ag matrix including the dislocations nucleating and emitted from the interface (corresponding to "1") and the dislocations propagating through the interface (corresponding to "2"). Due to the small difference in SFE between Cu and Ag,[52] the width of stacking faults of the Ag matrix is close to that of Cu nanofilm. With the further indentation, lots of dislocation loops appear in the Ag matrix (Fig. 3(i)). Eventually, the loops disappear in the lower surface of Cu/Ag multilayers, which is a similar phenomenon to that in bulk single-crystal Cu.

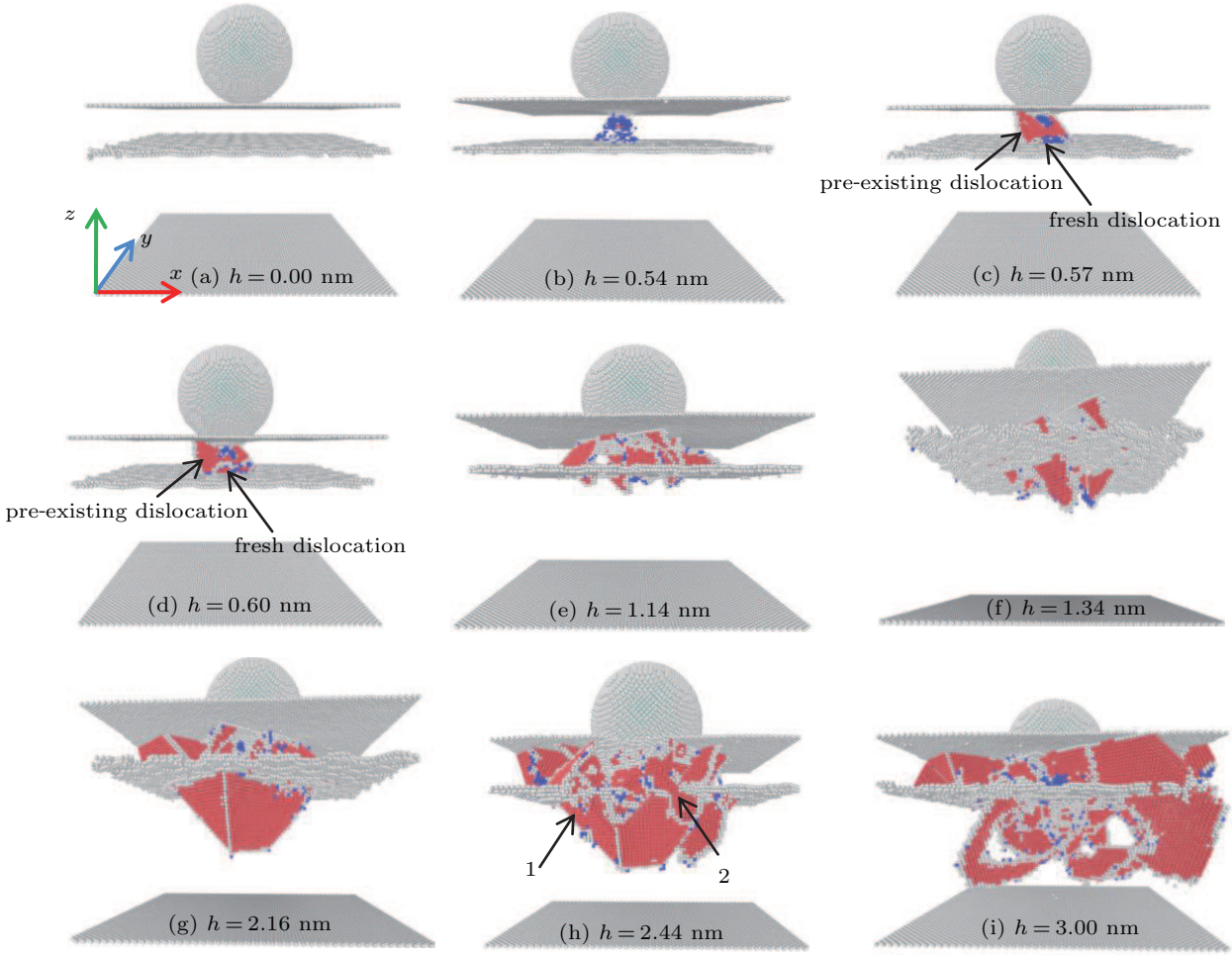


Fig. 3. (color online) Evolution processes of internal defects in Cu/Ag multilayers in the nanoindentation process.

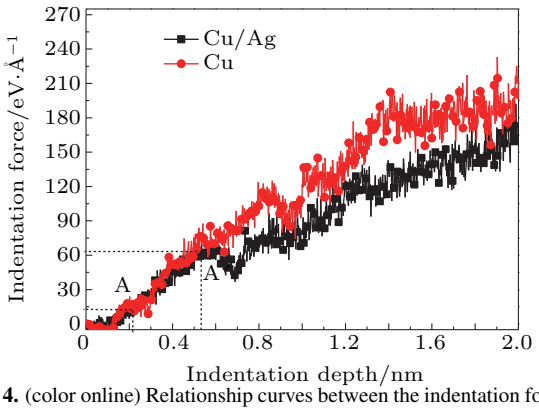


Fig. 4. (color online) Relationship curves between the indentation force and the indentation depth.

Figure 4 shows the relationship curves between indentation depth and indentation forces in Cu/Ag multilayers and bulk single-crystal Cu. Here, point "A" corresponds to Fig. 2(b), and point "A" corresponds to Fig. 3(b). It can be seen from Fig. 4 that due to the elastic deformation of Cu/Ag multilayers and bulk single-crystal Cu, the indentation forces increase linearly with the increase of the indentation depth at the beginning stage. However, the elastic deformation stage of Cu/Ag multilayers is longer than that of bulk single-crystal Cu by comparing OA' and OA segments, which implies that the incipient plastic deformation of Cu/Ag multilayers is postponed. It can be explained by the fact that due to the presence of the interface, the incipient dislocation nucleation and emission in Cu nanofilm are postponed during the nanoindentation of Cu/Ag multilayers. The indentation forces in Cu/Ag multilayers and bulk single-crystal Cu decrease in the transition

from the elastic deformation stage to the plastic deformation stage, because the dislocations slip under the indenter at this time, which can also explain the fluctuation of the indentation forces. The decline of the two curves also reveals that bulk single-crystal Cu and Cu/Ag multilayers have similar deformation mechanisms in the incipient plasticity stage, which is consistent with the results shown in Figs. 2(b) and 3(b).

4. Discussion

4.1. Effect of the lattice mismatch

The SFEs of Cu, Ag and Ni $E_{\mathrm{Cu}} = 56$ mJ/m^2, $E_{\mathrm{Ag}} = 34$ mJ/m^2, and $E_{\mathrm{Ni}} = 187$ mJ/m^2, respectively.[52] The differences η_1 and η_2 are obtained from the following expressions:

$$\eta_1 = E_{\mathrm{Cu}} - E_{\mathrm{Ag}} = 22\ \mathrm{mJ/m^2}, \tag{1}$$

$$\eta_2 = E_{\mathrm{Ni}} - E_{\mathrm{Cu}} = 131\ \mathrm{mJ/m^2}. \tag{2}$$

The lattice constants of fcc-Cu, fcc-Ag and fcc-Ni $a_{\mathrm{Cu}} = 3.62$ Å, $a_{\mathrm{Ag}} = 4.09$ Å, and $a_{\mathrm{Ni}} = 3.52$ Å, respectively.[41] The lattice mismatches in Cu/Ag multilayers and Ni/Cu multilayers δ_1 and δ_2 are obtained from the following expressions:

$$\delta_1 = \left|\frac{a_{\mathrm{Ag}} - a_{\mathrm{Cu}}}{a_{\mathrm{Cu}}}\right| = \left|\frac{4.09 - 3.62}{3.62}\right| \approx 0.13, \tag{3}$$

$$\delta_2 = \left|\frac{a_{\mathrm{Cu}} - a_{\mathrm{Ni}}}{a_{\mathrm{Ni}}}\right| = \left|\frac{3.62 - 3.52}{3.52}\right| \approx 0.03, \tag{4}$$

where η_1 and η_2 indicate that the difference of SFE between Cu and Ag is far smaller than that of SFE between Ni and Cu. The δ_1 and δ_2 display that the lattice mismatch of Cu/Ag multilayers is far larger than that of Ni/Cu multilayers. In addition, the width of stacking faults in the Ag matrix is approximately the same as that of stacking faults in Cu nanofilm during the plastic deformation of Cu/Ag multilayers. However, the partial dislocations widen in Cu after they have propagated through the interface during the plastic deformation of Ni/Cu multilayers.[25] These different phenomena during the plastic deformation of Cu/Ag multilayers and Ni/Cu multilayers can be explained by the fact that the difference of SFE between Cu and Ag is far smaller than that of SFE between Ni and Cu. Therefore, the plastic deformation of Cu/Ag multilayers is affected by the lattice mismatch more than by the difference of SFE between Cu and Ag.

Figures 5(a) and 5(b) show top views of the instantaneous state of the mismatch dislocation network before deformation and after deformation, respectively. Comparing the region "a" with region "a'", it is obvious to see that due to the dislocation pile-up at the interface, the mismatch dislocation network deforms due to the length change of the mismatch dislocations on the x–y plane. The length change of the mismatch dislocations causes the interface energy to increase and the energy to decrease, promoting the dislocation motion. Therefore, it is difficult for the dislocations to pass through the interface, and the dislocations nucleate and are emitted from the interface in order to release the interface energy.

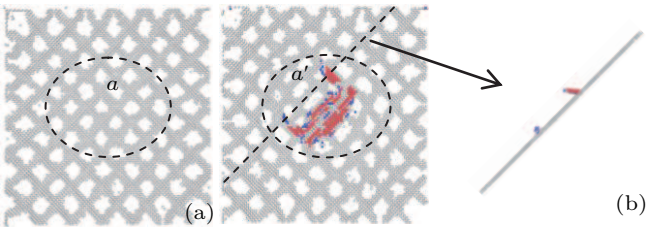


Fig. 5. (color online) Morphologies of the mismatch dislocation network in Cu/Ag multilayers (a) before deformation and (b) after deformation.

4.2. Effect of image force

Since the elastic moduli of Cu and Ag are different, there is the image force on the interface of Cu/Ag multilayers to attract or repel the dislocations. When the image force is negative, it means that the attractive force drives the dislocations through the interface, otherwise, it means that the repulsive force hinders the dislocations from crossing the interface. For Cu/Ag multilayers, the image force acting on the dislocations inside Cu nanofilm is described by the following equation:

$$F_i = \frac{\left(E_{\mathrm{Ag}} - E_{\mathrm{Cu}}\right) E_{\mathrm{Cu}} b^2}{\left(E_{\mathrm{Ag}} + E_{\mathrm{Cu}}\right) 4\pi c} \frac{h_{\mathrm{Cu}} - 2c}{h_{\mathrm{Cu}} - c} \sin\theta, \tag{5}$$

where E_{Cu} and E_{Ag} are the elastic moduli of Cu and Ag, and $E_{\mathrm{Cu}} > E_{\mathrm{Ag}}$;[53] b is the modulus of the Burgers vector of dislocations inside Cu nanofilm; h_{Cu} is the thickness of the Cu nanofilm, and h_{Cu} is taken to be 3 nm; c is the distance between the dislocations and the interface, here, the dislocations are near to the interface, namely $h_{\mathrm{Cu}} > 2c$. The angle between the slip surfaces of the dislocations and the interface is θ.

It can be obtained from Eq. (1) that the image force is a certain attraction to the dislocations of Cu nanofilm. In addition, it is determined above that the mismatch dislocation network has a great resistance to the dislocation motion. However, figure 3 shows that most of the dislocations pile on the interface, which indicates that the dislocation pile-up at the interface is determined by the obstruction of the mismatch dislocation network and the attraction of the image force. If the indentation force continues to increase, more dislocations will pile-up at the interface and the mismatch dislocation network will deform more seriously, which will cause the interface stress and interface energy to increase.[51] When the stresses and energy reach their critical values, the dislocations nucleate and are emited into the Cu nanofilm and the Ag matrix, which is consistent with the result shown in Fig. 3.

5. Conclusions

In summary, the three-dimensional MD simulations are conducted to investigate the plastic deformation mechanism of Cu/Ag multilayers in the nanoindentation process. Based on the above discussion, conclusions can be obtained as outlined below.

When the dislocations reach the interface, the dislocations pile-up at the interface and then the plastic deformation of the Ag matrix occurs by the nucleation and emission of dislocations from the interface and the dislocation propagation through the interface. In addition, due to the presence of the interface, the incipient plastic deformation of Cu/Ag multilayers is postponed, compared with that of bulk single-crystal Cu. The plastic deformation of Cu/Ag multilayers is affected by the lattice mismatch more than by the difference of SFE between Cu and Ag. Furthermore, the dislocation pile-up at the interface is determined by the obstruction of the mismatch dislocation network and the attraction of the image force.

It is worth noting that the nucleation and emission of dislocations from the interface and the dislocation propagation through the interface are observed during the plastic deformation of Cu/Ag multilayers. However, in the previous studies of Ni/Cu and Ni/Al multilayers, only the dislocation propagation through the interface occurs, and the nucleation and emission of dislocations from the interface are hardly observed.[25,27,54]

References

[1] Misra A, Verdier M, Lu YC, Kung H, Mitchll T E, Nastasi M and Embury J D 1998 *Scr. Mater.* **39** 555
[2] Clemens B M, Kung H and Barnett S A 1999 *MRS Bull.* **24** 20
[3] Bufford D, Bi Z, Jia Q X, Wang H and Zhang X 2012 *Appl. Phys. Lett.* **101** 223112
[4] Misra A, Kung H, Embury J D 2004 *Scr. Mater.* **50** 707
[5] Mara N A, Bhattacharyya D, Dickerson P, Hoagland R G and Misra A 2008 *Appl. Phys. Lett.* **92** 231901
[6] Mara N A, Bhattacharyya D, Dickerson P O, Hoagland R G and Misra A 2009 *Mater. Sci. Forum* **633–634** 647
[7] Misra A, Zhang X, Hammon D and Hoagland R G 2005 *Acta Mater.* **53** 221
[8] Zhang J Y, Zhang X, Wang R H, Lei S Y, Zhang P, Niu J J, Liu G, Zhang G J and Sun J 2011 *Acta Mater.* **59** 7368
[9] Was G S and Foecke T 1996 *Thin Solid Films* **286** 1
[10] Misra A, Kung H and Embury J D 2004 *Scr. Mater.* **50** 707
[11] Gao X M, Sun J Y, Hu M, Weng L J, Zhou F and Liu W M 2011 *Appl. Surf. Sci.* **257** 7643
[12] Benghalem A and Morris D G 1997 *Acta Mater.* **45** 397
[13] Han K, Lawson A C, Wood J T, Embury J D, Von Dreele R B and Richardson Jr J W 2004 *Philos. Mag.* **84** 2579
[14] Hansen N 2004 *Scr. Mater.* **51** 801
[15] Furukawa M, Horita Z, Nemoto M, Valiev R Z and Langdon T G 1996 *Acta Mater.* **44** 4619
[16] Was G S and Foecke T 1996 *Thin Solid Films* **286** 1
[17] Wang J, Hoagland R G, and Misra A 2009 *Scr. Mater.* **60** 1067
[18] Misra A, Hirth J P and Kung H 2002 *Philos. Mag. A* **82** 2935
[19] Fang Q H, Liu Y W, Jin B and Wen P H 2009 *Int. J. Solids Struct.* **46** 1413
[20] Liu Y W and Fang Q H 2007 *Mat. Sci. Eng. A* **464** 117
[21] Zhao Y X, Zeng X and Chen C P 2014 *Chin. Phys. B* **23** 030202
[22] Li J, Liu B, Fang Q H, Huang Z W and Liu Y W 2017 *Ceram. Int.* **43** 3839
[23] Li J, Guo J W, Luo H, Fang Q H, Wu H, Zhang L C and Liu Y W 2016 *Appl. Surf. Sci.* **364** 190
[24] Li J, Fang Q H, Liu Y W and Zhang L C 2014 *Appl. Surf. Sci.* **303** 331
[25] Shao S and Medyanik S N 2010 *Mech. Res. Commun.* **37** 315
[26] Zhang J J, Wang Z F, Yan Y D and Sun T 2016 *RSC Adv.* **6** 59206
[27] Cao Y Z, Zhang J J, Liang Y C, Yu F L and Sun T 2010 *Appl. Surf. Sci.* **257** 847
[28] Wen S P, Zong R L, Zeng F, Gao Y and Pan F 2007 *J. Mater. Res.* **22** 3423
[29] Cai W and Bellon P 2013 *Wear* **303** 602
[30] Verdier M, Huang H, Spaepen F, Embury J D and Kung H 2006 *Philos. Mag.* **86** 5009
[31] McKeown J, Misra A, Kung H, Hoagland R G and Nastasi M 2002 *Scr. Mater.* **46** 593
[32] Pei Q X, Lu C, Lee H P and Zhang Y W 2009 *Nanoscale Res. Lett.* **4** 444
[33] Zhang G, Guo J, Ming W, Huang Y, Shao X and Zhang Z 2014 *Appl. Surf. Sci.* **290** 359
[34] Tong Z, Liang Y C, Jiang X Q and Luo X C 2014 *Appl. Surf. Sci.* **290** 458
[35] Zhang B, Zheng X, Tokura H and Yoshikawa M 2003 *J. Mater. Process. Tech.* **132** 353
[36] Yan J, Asami T, Harada H and Kuriyagawa T 2009 *Precis. Eng.* **33** 378
[37] Wadley H N G, Zhou X, Johnson R A and Neurock M 2001 *Prog. Mater. Sci.* **46** 329
[38] Cheng D, Yan Z J, Yan L 2007 *Thin Solid Films* **515** 3698
[39] Mylvaganam K, Zhang L C, Eyben P, Mody J and Vandervorst W 2009 *Nanotechnology* **20** 305705
[40] Zhang J J, Sun T, Yan Y and Liang Y 2009 *Mater. Sci. Eng. A* **505** 65
[41] Foiles S M, Baskes M I and Daw M S 1986 *Phys. Rev. B* **33** 7983
[42] Daw M S, Foiles SM and Baskes M I 1993 *Mater. Sci. Rep.* **9** 251
[43] Zhou X W, Wadley H N G and Johnson R A 2001 *Acta Mater.* **49** 4005
[44] Pei Q X, Lu C and Lee H P 2010 *Comp. Mater. Sci.* **41** 177
[45] Pei Q X, Lu C, Fang F Z and Wu H 2006 *Comp. Mater. Sci.* **37** 434
[46] Zhang J J, Sun T, Yan Y D, Liang Y C and Dong S 2009 *Appl. Phys. A* **94** 593
[47] Plimpton S J 1995 *J. Comp. Phys.* **117** 1
[48] Stukowski A 2010 *Model. Simul. Mater. Sci.* **18** 015012
[49] Honeycutt J D and Andersen H C 1987 *J. Phys. Chem.* **91** 4950
[50] Liu X M, Liu Z L and Wei Y G 2012 *Tribol. Lett.* **46** 167
[51] Capolungo L, Spearot D E, Cherkaoui M, McDowell D L, Qu J and Jacob K I 2007 *J. Mech. Phys. Solids* **55** 2300
[52] Rosengaard N M and Skriver H L 1993 *Phys. Rev. B* **47** 12865
[53] Yu Y N 2003 *Principles of Metallography* (Beijing: Metallurgieal Indsutry Press)
[54] Saraev D and Miller R E 2006 *Acta Mater.* **54** 33